Computational & Multiscale
Mechanics of Materials

Building, Architecture and Town
Planning

CM3
www.ltas-cm3.ulg.ac.be

BATiR
www.batir.ulb.ac.be

Generation and Analysis of open foam RVEs with sharp edges using Distance fields and Level sets

Nanda G. Kilingar
K. Ehab Moustafa Kamel
B. Sonon
L. Noëls
T.J. Massart

Kilingar, N. G., et al, Generation of Open-foam Representational Volume Elements using distance fields and level sets, *Under preparation*

Contents

- Open foam materials, properties and existing models
- DN-RSA based packing generation
  - DN-RSA Notation
  - Tessellation Generation
- Open foam morphology
- Sharp Edge extraction
  - Multiple level set method
  - Inner level set extraction
  - 3D Open Foam model
- Strut cross section variation
- Properties of the RVEs generated
- Numerical analysis
- Limitations and advantages

Open foam materials and properties

- Metallic open foams
  - Low density
  - Novel physical, mechanical and acoustic properties.
  - Offer potential for lightweight structures, with high stiffness and energy absorption capability.
  - With advancing manufacturing capabilities, they are becoming more affordable.
- Ability to model 3D foams based on actual foam samples
  - Helps in characterization
  - Stochastic approaches and multi-scale mechanics used to simulate the behavior

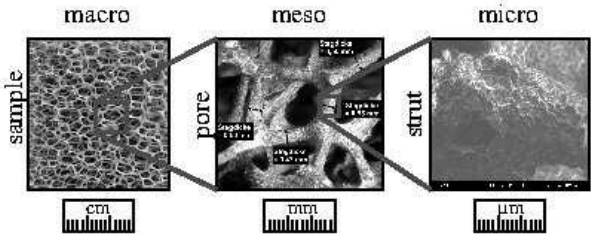

Jung & Diebels 2014

- Manufacturing (Zhou et al 2002)
  - PU foam → phenomenon of bubble expansion
  - Metallic foam → PU foams + casting/ electrodeposition
- Plateau's law (Sonon et al 2015)
  - Soap bubble → Plateau's law, Surface energy minimization
    - Constant mean curvature of each face
    - 3 faces meet at 120^0, equal dihedral angles
    - 4 edges join at equal tetrahedral angles (109.47^0)

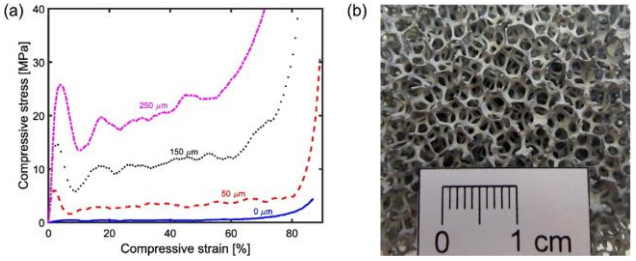

Jung et al 2015

Numerical approach and DN-RSA

- Regular models
  - Kelvin's tetrakaidecahedra (1887)
  - Weaire-Phelan cell (1993)
- Tessellations of sphere packing distribution – Laguerre tessellations
  - Sphere packing generation
    - Concurrent or force-biased approach (Ex, Stroeven 1996)
    - Sequential approach (Ex, RSA, Cooper 1988)
  - Tessellation generated by methods like convex hull (QHull, Barer et al 1996)
  - Morphological parameters like face-by-cell count, edge-by-face count, interior angles match very well
- DN-RSA: Distance neighbor based random sequential packing algorithm for arbitrary shaped iniclusions (Sonon et al 2012)

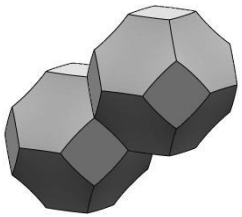

Kelvin cell

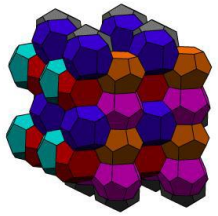

Weaire-Phelan modification

- Too regular
- Fail to represent non-uniform bubble sizes and out-of-equilibrium solid foams.

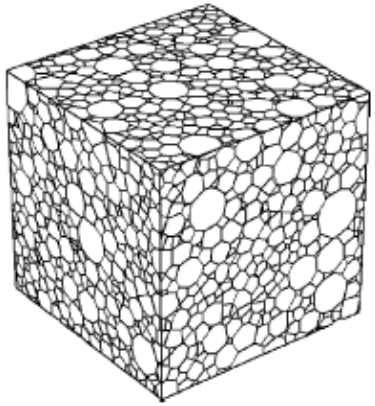

Random close packing of spheres based Laguerre Voronoï diagram (Fan et al 2004)

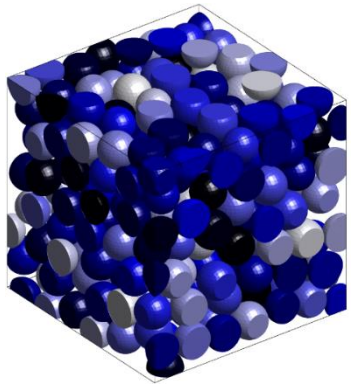

DN-RSA Notation

- Inclusions from desired distribution/shape are generated and placed in the domain.
  - Each grid point assigned a $DN_k(\boldsymbol{x})$ value, k - the kth nearest inclusion to the given point.
- $DN_k(\boldsymbol{x})$
  - negative inside the inclusion
  - positive outside.
- With addition of more inclusions, the $DN_k(\boldsymbol{x})$ value gets updated, depending on the k-th nearest inclusion and this inclusion mapping is stored as $NN_k(\boldsymbol{x})$.

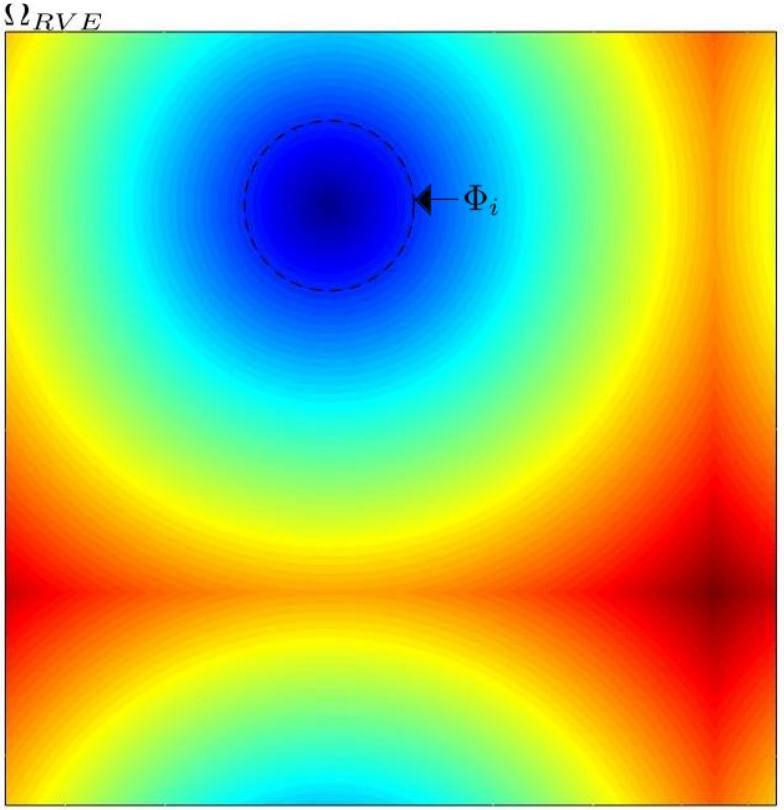

$DN_1(\boldsymbol{x})$ plot with only 1 inclusion

Generation of Tessellation

- Tessellation
  - Assembly of all domains ${}^{I}\Theta_i$ that enclose, for each inclusion i, points closer to this inclusion than to others, i.e., $NN_1(\boldsymbol{x}) = i$.
- Implicitly extracted in DN-RSA by "Voronoï" level set function:
  - $O_V(\boldsymbol{x}) = DN_2(\boldsymbol{x}) - DN_1(\boldsymbol{x})$
- A closed cell geometry can be extracted using a quasi-constant thickness, *t*:
  - $O_v(\boldsymbol{x}) - t = 0$

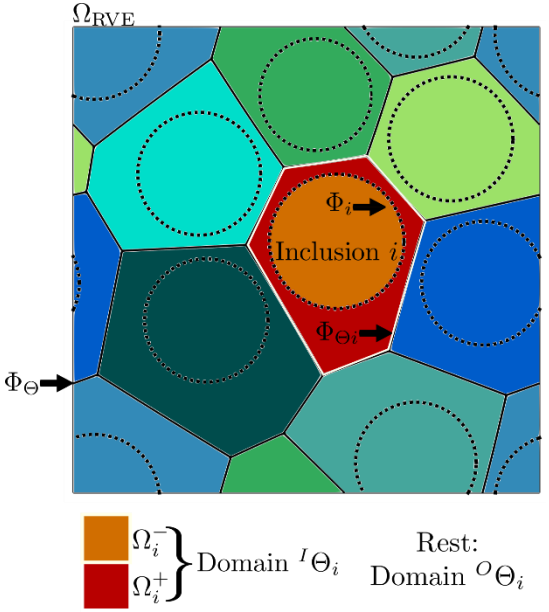

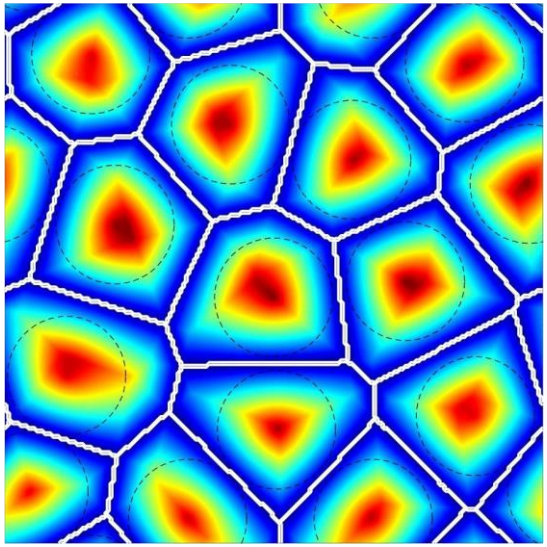

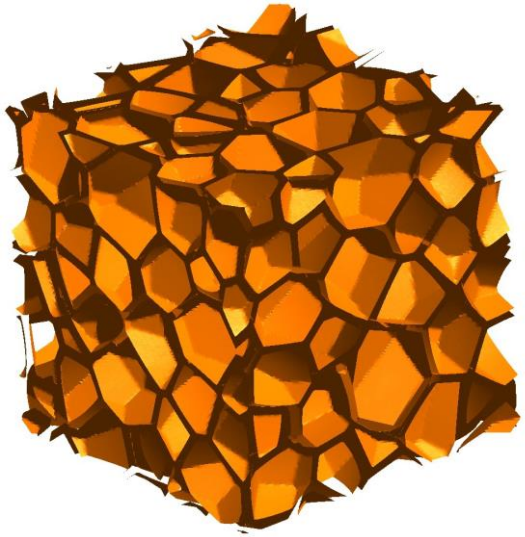

Open foam morphology

- Plateau borders in liquid foams form at the intersection of three films. Thus we combine the 3 first neighbor distance functions.
- “Plateau” Level set function
  - $O_P(\boldsymbol{x}) = \frac{DN_3(\boldsymbol{x})+DN_2(\boldsymbol{x})}{2} - DN_1(\boldsymbol{x})$
- Function consists of triangles with vertex lying on the tessellation cell boundaries.
- Thus, we can extract plateau border like geometry through
  - $O_P(\boldsymbol{x}) - t = 0$
  - Parameter t used to control thickness of extracted borders

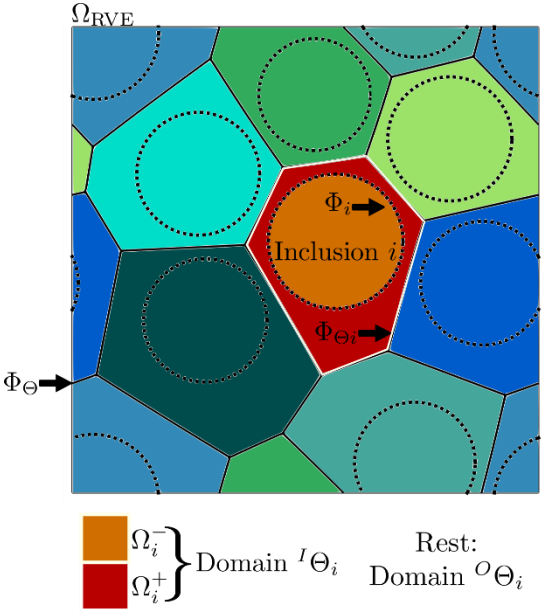

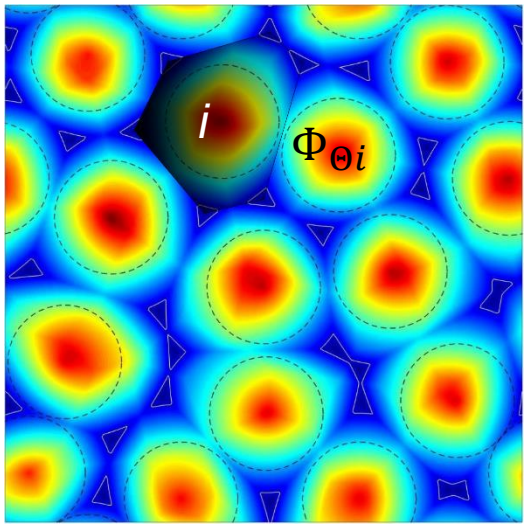

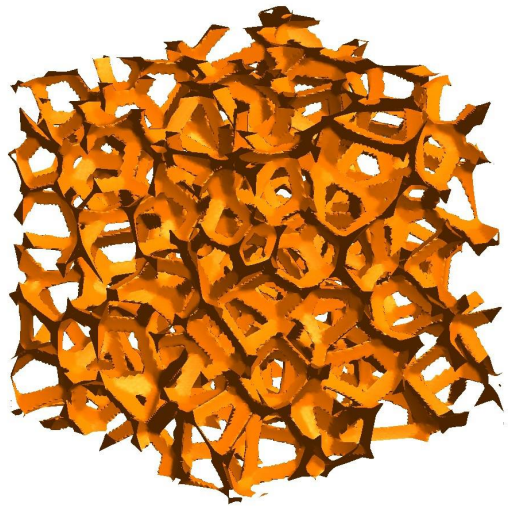

Sharp edge extraction

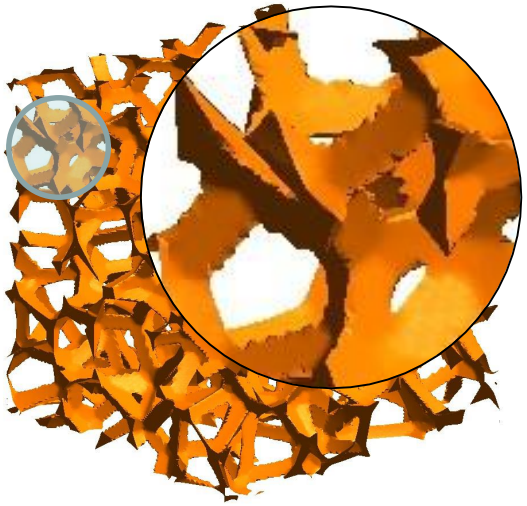

- Plateau borders present sharp edges due to their triangular prism shape
  - Origin is due to steep discontinuity of $DN_k(\boldsymbol{x})$ derivatives on Φ_Θ
- Single level set function can not represent this with discrete level set functions, and we need multiple level set function strategy

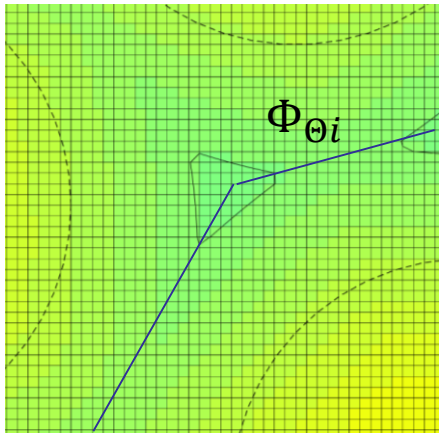

t Level Set

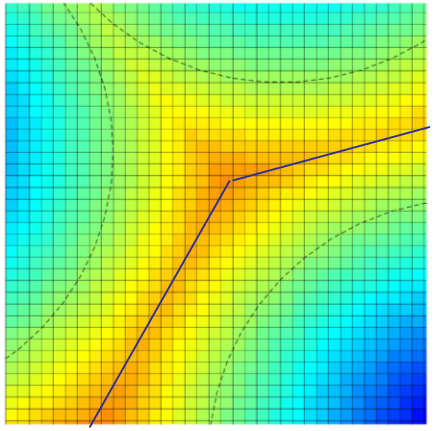

$DN_1(\boldsymbol{x})$

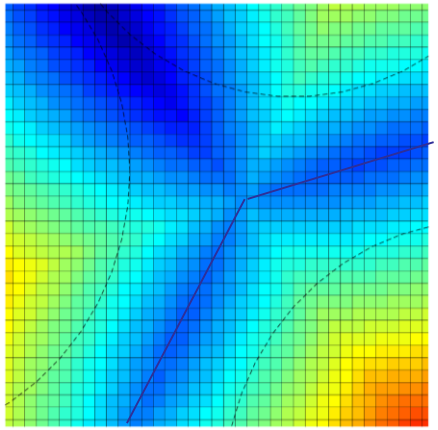

$DN_2(\boldsymbol{x})$

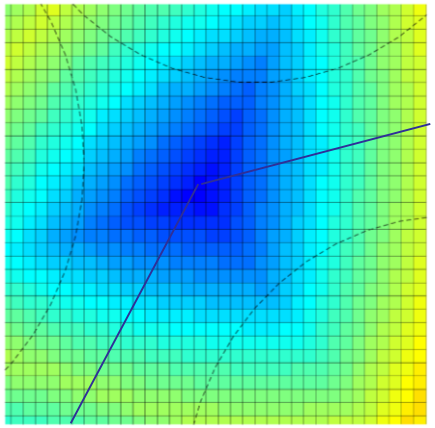

$DN_3(\boldsymbol{x})$

Clipping of the triangular section at grid positions and the presence of discontinuities in $DN_1(\boldsymbol{x})$ and $DN_2(\boldsymbol{x})$ across Φ_Θ. $DN_3(\boldsymbol{x})$ is continuous.

Sharp edge extraction – Multiple level set functions

- Local level set functions for each inclusion, ${}^{I}O_P(\boldsymbol{x})$ → Global "Plateau" function, $O_P(\boldsymbol{x})$ + modified $DN_k(\boldsymbol{x})$
  - Local functions are built for each inclusion from modified $DN_k(\boldsymbol{x})$, called ${}^{I}DN_{ki}(\boldsymbol{x})$ only in the domain $NN_k(\boldsymbol{x}) = i,\ k = \{1,2,3\}$.

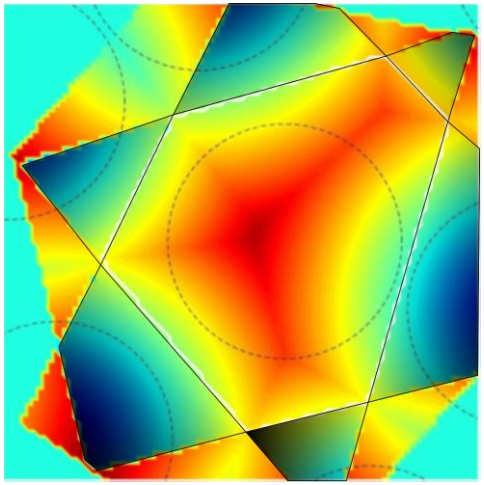

$$ {}^{I}DN_{2i}(\boldsymbol{x}) = \begin{cases} DN_2(\boldsymbol{x}), & NN_2(\boldsymbol{x}) \neq i \\ DN_1(\boldsymbol{x}), & NN_2(\boldsymbol{x}) = i \end{cases} $$

$NN_2(\boldsymbol{x}) = i$ is the shaded domain

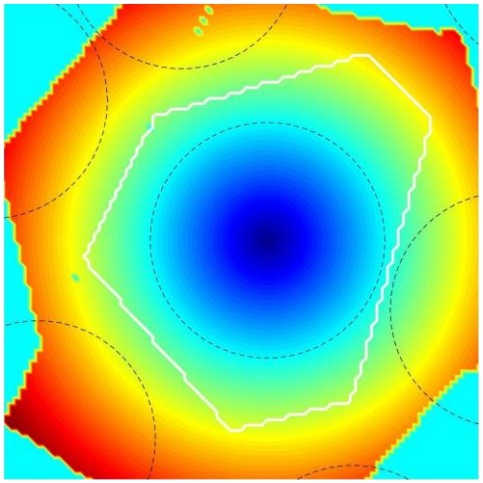

$${}^{I}DN_{1i}(\boldsymbol{x}) = DS_i(\boldsymbol{x})$$

$DS_i(\boldsymbol{x})$ is the signed distance field of the domain for inclusion i

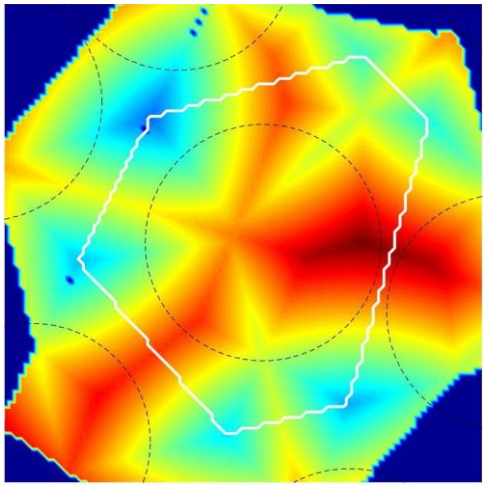

$${}^{I}DN_{3i}(\boldsymbol{x}) = DN_3(\boldsymbol{x})$$

$DN_3(\boldsymbol{x})$ is continuous across Φ_Θ

Sharp Edge Extraction – “Inner” Level Set function

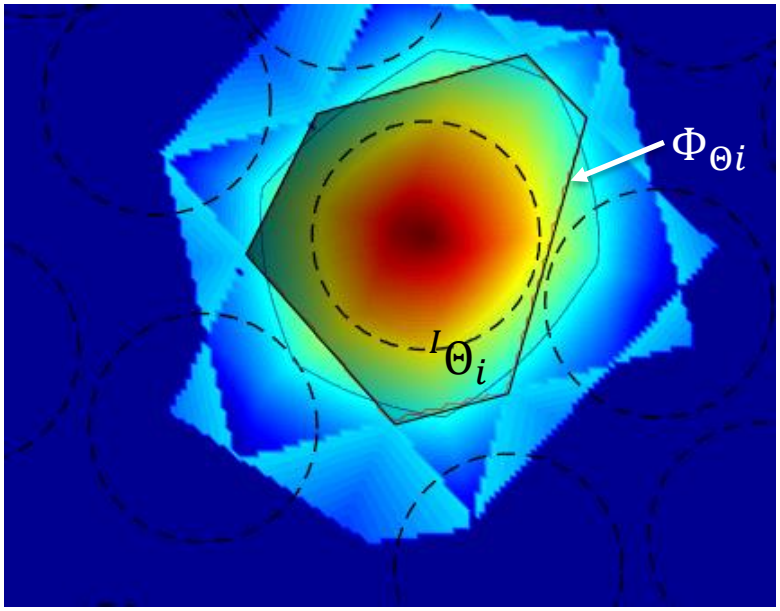

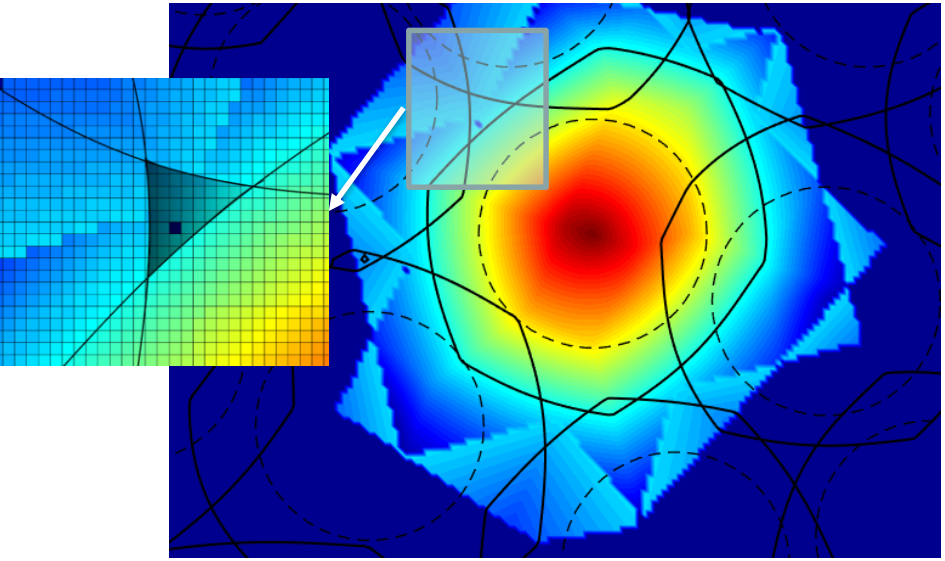

- ${}^{I}O_{Pi}(\boldsymbol{x})$ function, with t level set, C^1 continuous across $\Phi_{\Theta i}$ and equal to global function $O_P(\boldsymbol{x})$ in domain ${}^{I}\Theta_i$.
- The value of ${}^{I}O_{Pi}(\boldsymbol{x})$ is positive towards the center of the inclusion and negative outside.
- The t level set is stored for individual inclusion.
- The t level set of inclusion i is iteratively compared with t level sets of the neighboring inclusions.
- Segments of t lying such that ${}^{I}O_{Pj}(\boldsymbol{x}) > 0, j \neq i$ are sliced off.

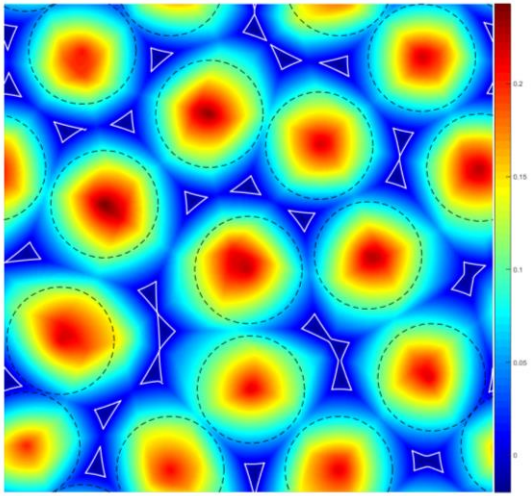

Sharp Edge extraction

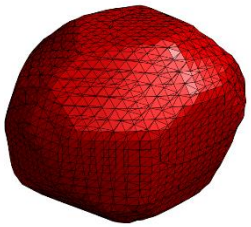

t level set of inclusion i extracted in MATLAB using $\boldsymbol{isosurface}$ function

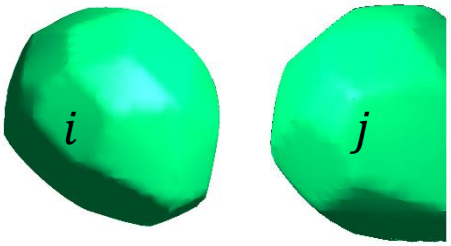

Intersection of t level sets of inclusion i and j by surface Boolean tool $Cork$

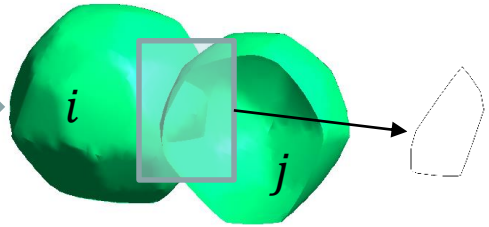

Extract, **re-mesh** and **fix** the line of intersection

Slice-off the elements lying in the domain ${}^{I}O_{Pj}(\boldsymbol{x}) > 0, j \neq i$

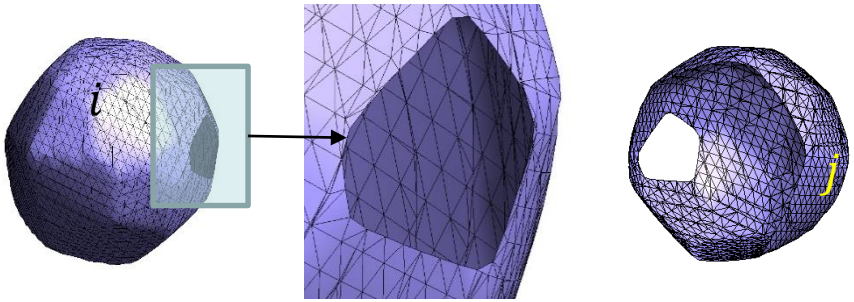

Similarly, **slice-off** the elements of t level set of inclusion j lying in the domain ${}^{I}O_{Pi}(\boldsymbol{x}) > 0, i \neq j$

Iteratively done, leaving only the plateau border part of the inclusion. Traditional *isosurface* operations result in ill-formed elements.

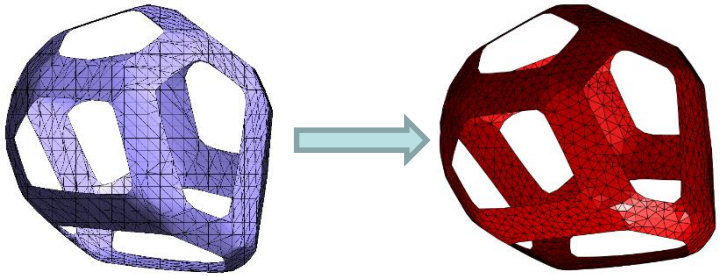

Inclusions are then refined by level set based mesh conforming approach designed by [Karim et al (under preparation)] using analogy of equilibrium of 3D truss system (Persson and Strang, 2004) before assembling. 3D mesh is generated using Tetgen (Hang Si 2015)

Strut cross section variation

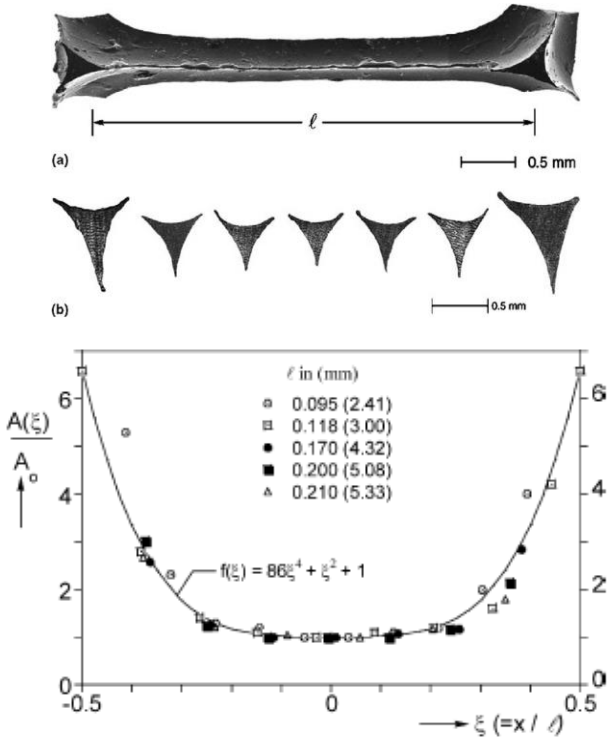

Strut cross section variation and mid-span cross-sectional area of a polyurethane foam; Gong et al 2004

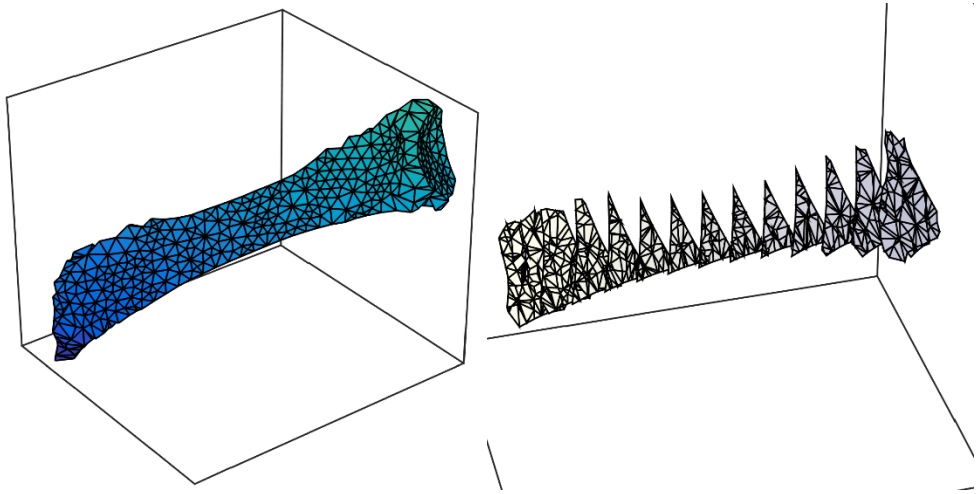

$$O_{S1}(\mathbf{x}) = DN_4(\mathbf{x}) - DN_3(\mathbf{x})$$

Value of the function increases from 0 at the intersection of struts to half the length of the strut at mid-span along the axis.

$$\Omega_{ijk} = (NN_1(\mathbf{x}) = i)\&(NN_2(\mathbf{x}) = j)\&(NN_3(\mathbf{x}) = k)$$

Tetrahedral domain joining the center of the inclusion *I,* center of the common face between *I* and *j*, and the two ends of the strut formed by *I*, *j*, and *k*

DN-RSA is able to incorporate these variations by modifying the “Plateau” function O_P according to the domain using DN_3 and DN_4.

Strut cross section variation

$$\xi' = \frac{O_{S1}(\Omega_{ijk})}{\max(O_{S1}(\Omega_{ijk}))}$$

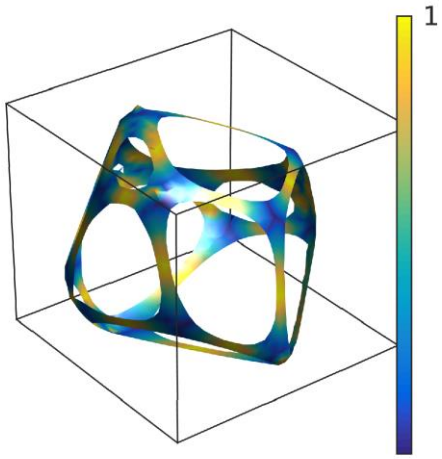

$$O_S(\mathbf{x}) = \sqrt{\frac{A(\xi')}{A_0}}$$

$$O_P(\mathbf{x}) - tO_s(\mathbf{x}) = 0$$

The final operator and the equation that enables to generate variation in strut cross-section

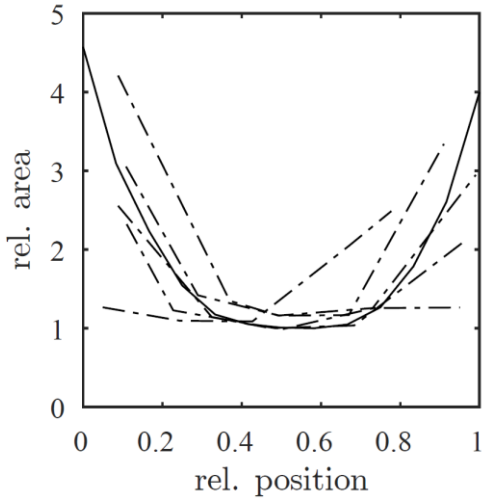

- Dotted line – strut cross section area data from 20ppi foam sample from Jung and Diebels 2017
- Bold line – data from a simulated 20ppi foam using DN-RSA

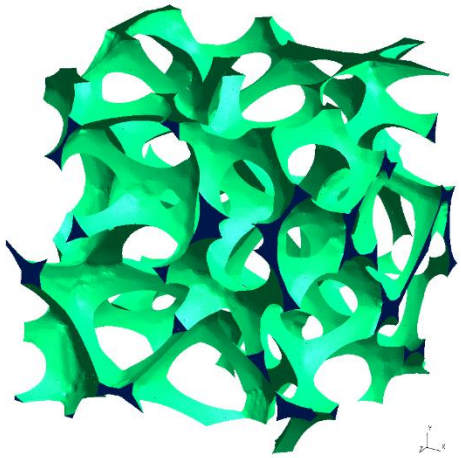

An RVE simulating a 20ppi foam with 25 inclusions

Morphology Characterization

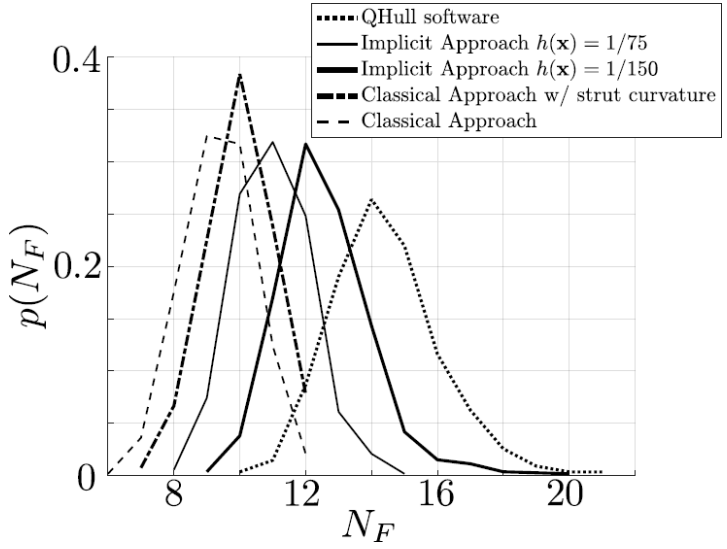

No. of faces per cell

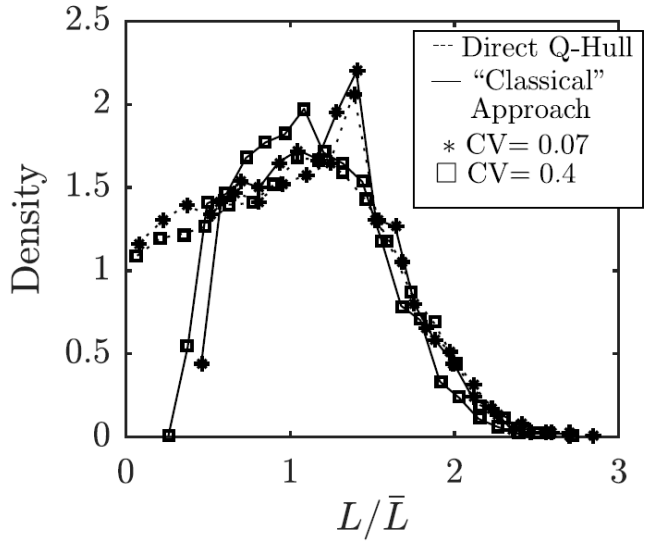

Strut length

- Classical Approach – Using the triangulated surfaces extracted from level set contouring
- Implicit approach – Using the calculated functions like NN_k, DN_k, O_P, etc

The RVEs generated have a mean face per cell value ranging from 13.5 to 14.5 depending on the packing fraction of the sphere, lower the fraction, more irregularity in the RVE. [Redenbach et al 2009]

Typical high values found in Laguerre tessellations from QHull not obtained due to limitations of the discretization grid.

Strut length distribution from DN-RSA in comparison with QHull Laguerre tessellations show that the short edges get absorbed by the sharp edge extraction technique, mimicking the process of model extraction from (Van der Burg et al 1997)

Morphology Characterization

	Experimental values from literature		Values used in DN-RSA			
ppi	Porosity(%)	Average strut thickness to average radius of inclusion ratio, T/L	Average values of $[c_1\ c_2]$	Average value of k	T/L ratio for t :	Obtained porosity
5	-	0.2310	-	-	-	-
10	0.942	0.1945	[50 1]	0	0.2050	0.9418
20	0.937	0.1983	[25 1]	-0.05	0.2	0.9388
30	0.916	-	[10 1]	-0.2	0.198	0.92
40	-	0.1878	-	-	-	-

Jung & Diebels 2017 Perrot et al 2007

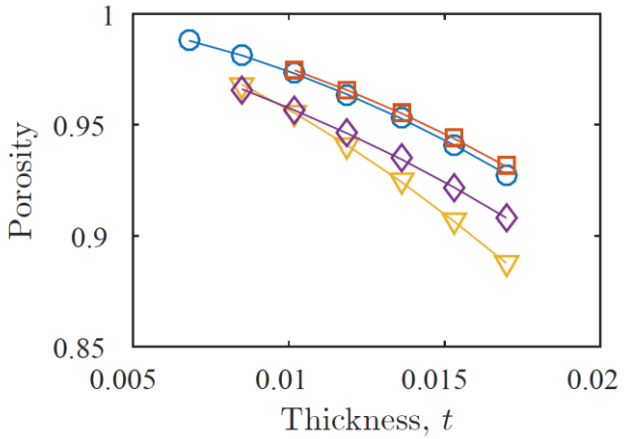

Variation of the RVE porosity with strut thickness and cross section variations; Legend
○ $c_1 = 20$
□ $c_1 = 60$, denoting thinner strut cross-section at mid strut
Δ $c_1 = 3$, denoting almost uniform cross-section, and
◊ $c_1 = 20$, $k = -0.5$ with convexity in the strut cross-section.

Numerical Simulation – Single pore

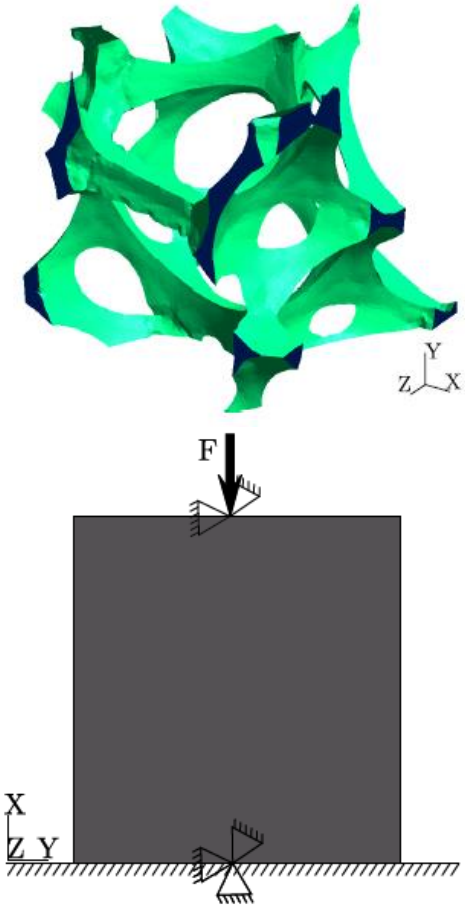

- Hyperelastic-based J2-elasto-plastic material law formulated in large strains (Nguyen & Noels 2014)
- $\sigma_y^0(\bar{\varepsilon}^{pl}) = \sigma_0 + H_{iso}\bar{\varepsilon}^{pl}$

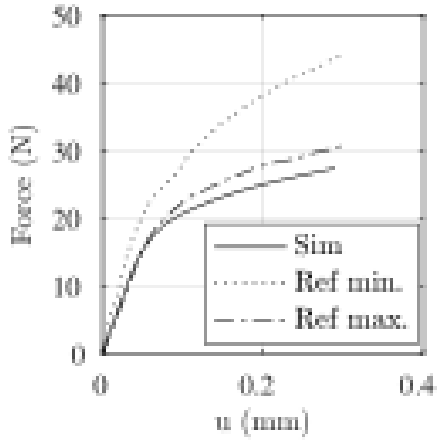

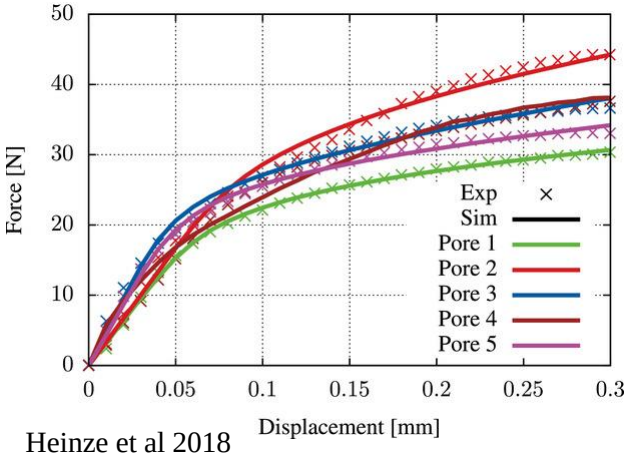

Heinze et al 2018

Numerical Simulation – RVE

- Larger RVE with 25 inclusions completely inside the domain.
- Uniaxial compression test comparison with experimental values; contact criteria not implemented.

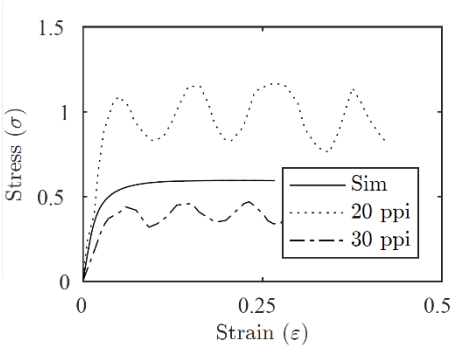

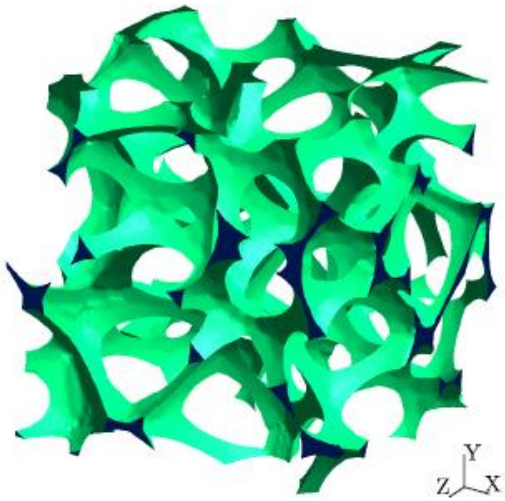

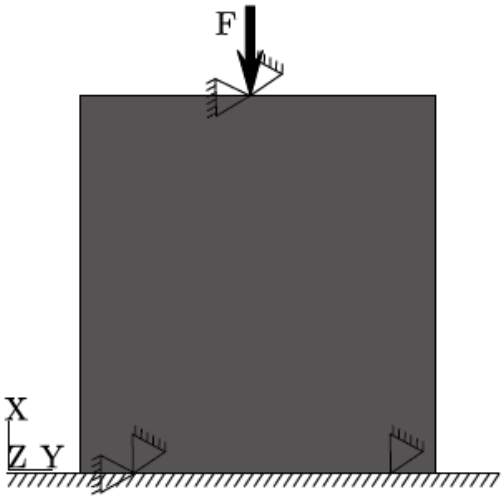

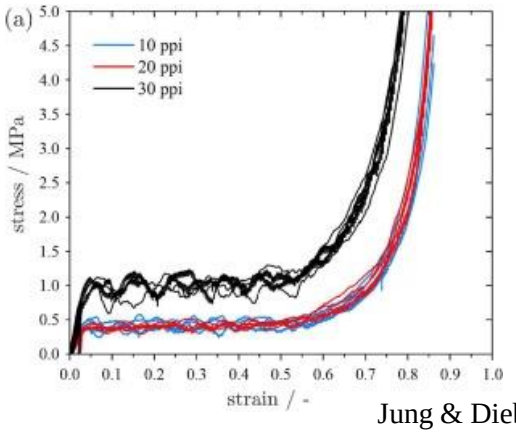

Jung & Diebels 2017

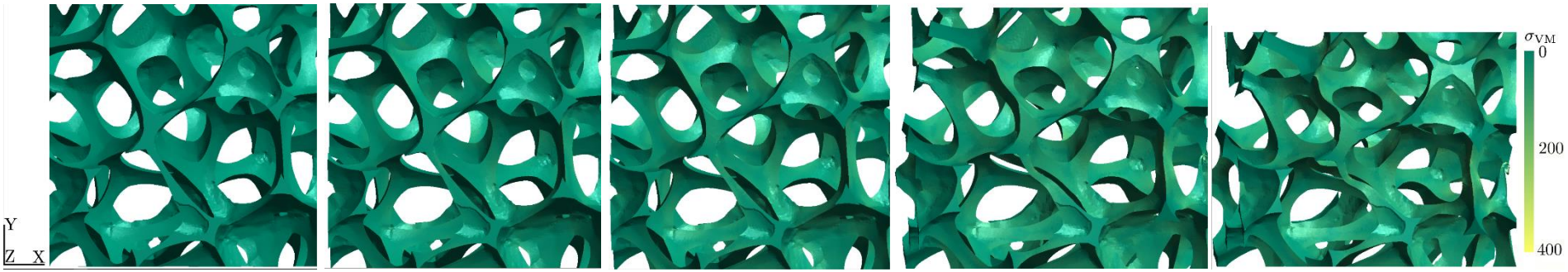

Further advantages of DN-RSA

- Periodic RVEs and RVEs with free boundary
- Strut cross-section concavity and convexity using concavity operators based on distance function
- Generation of RVEs with layers of coatings with non-smooth coatings using distance functions

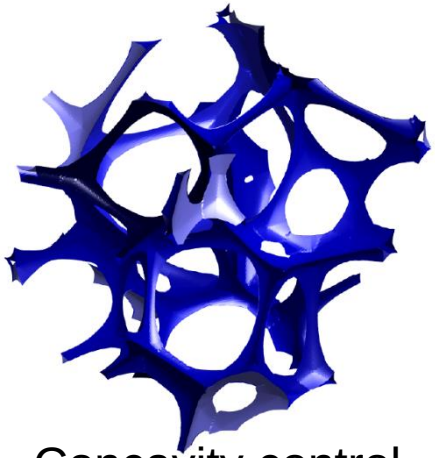

Concavity control

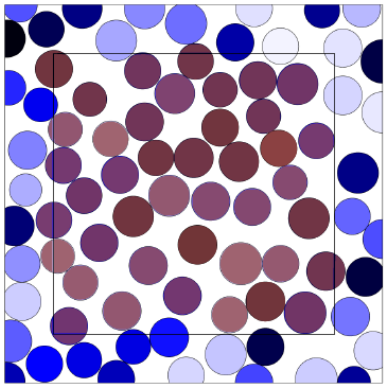

Free boundary RVE with minus sampling

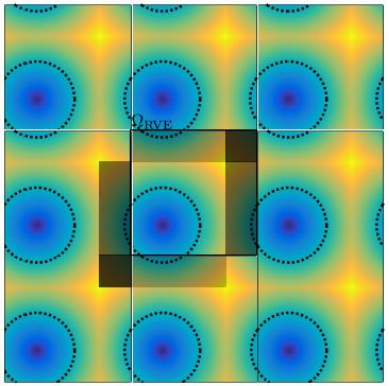

Periodicity in RVE

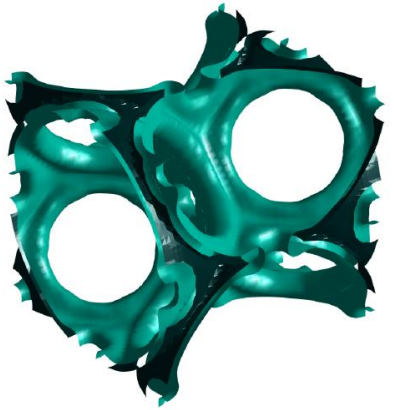

Layers of coatings

Limitations and Advantages

- **Higher discretization** of the grid required to capture higher sphere packing
- Laguerre tessellations are known to have higher number of **small struts** and **triangular faces** that are skewed,
  - captured by DN-RSA in the limit of vanishing discretization size.
- Representation of foams with RVE having high dispersion rate of the inclusion size is difficult with this model due to the necessary discretization grid.

- Easy access to **the signed distance functions** allows us to implement variations in the morphology
  - strut cross-section variation at the mid-span and along the axis of the strut
  - combination of open-closed faces of tessellated cells
  - Coating of the RVE to represent realistic engineering applications
- A balance of discretization size allows us to model the foam without the issues of small/skewed faces as they are implicitly enveloped by the extracted t level set.
- Extracted mesh can be easily utilized for **a multi-scale study** and understand the effects of upscaling the model to study the elastic-plastic properties of such foams

Thank you for your attention

Generation of open foam RVEs with sharp edges using Distance fields and Level sets

Nanda G. Kilingar, K. Ehab Moustafa Kamel, B. Sonon, L. Noëls, T.J. Massart

Computational & Multiscale Mechanics of Materials – CM3
http://www.ltas-cm3.ulg.ac.be/
B52 - Quartier Polytech 1
Allée de la découverte 9, B4000 Liège
ngkilingar@uliege.be

DN-RSA Notations

- $DN_k(\boldsymbol{x})$ is the k-th neighbor distance field

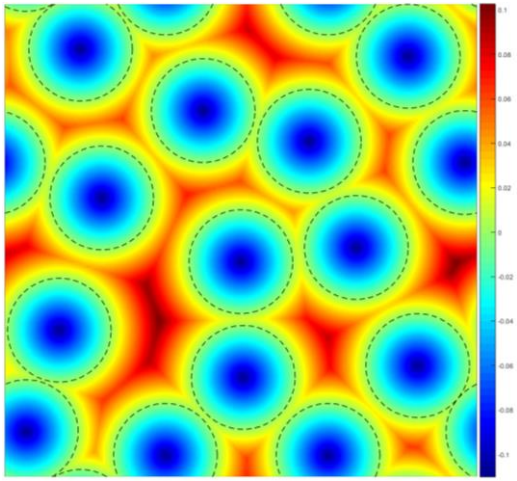

$DN_1(\boldsymbol{x})$

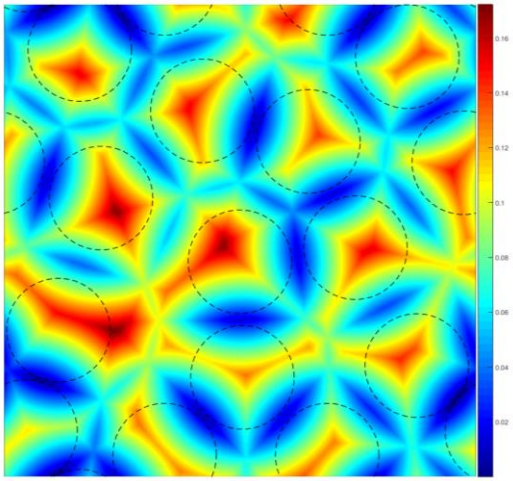

$DN_2(\boldsymbol{x})$

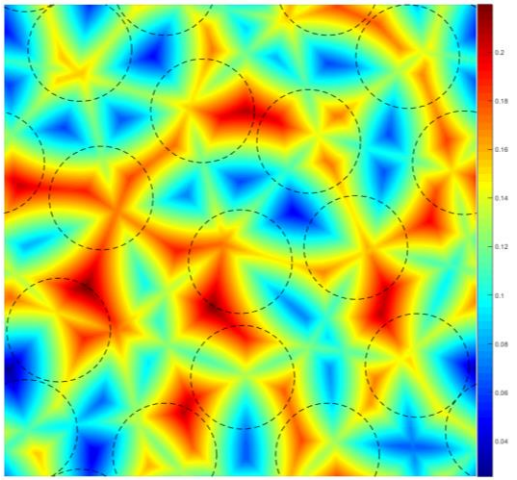

$DN_3(\boldsymbol{x})$

- $NN_k(\boldsymbol{x})$ is the k-th neighbor identity map

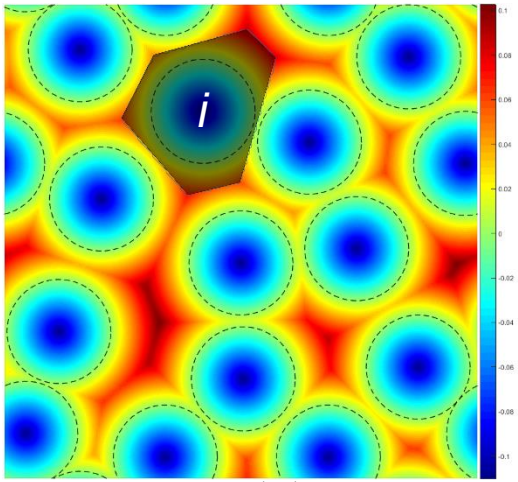

$NN_1(\boldsymbol{x}) = i$

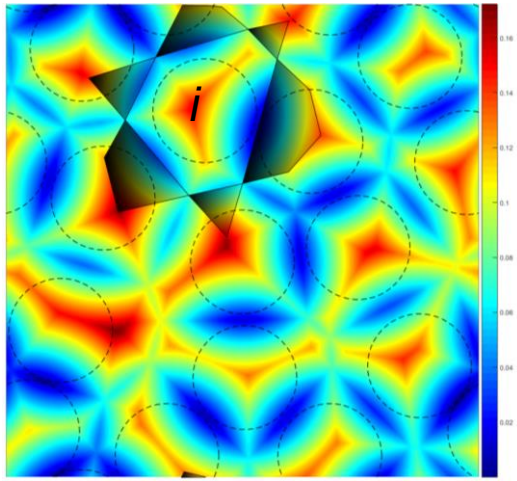

$NN_2(\boldsymbol{x}) = i$

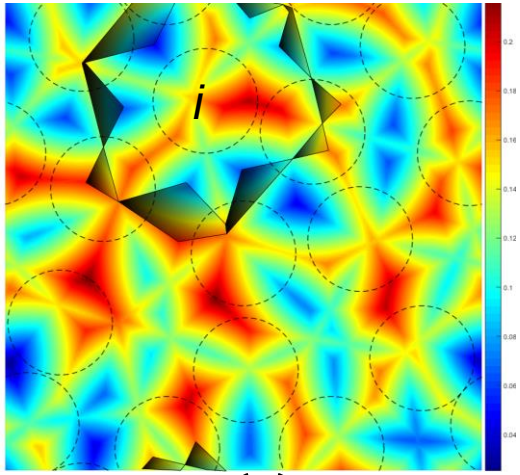

$NN_3(\boldsymbol{x}) = i$

Strut cross section variation

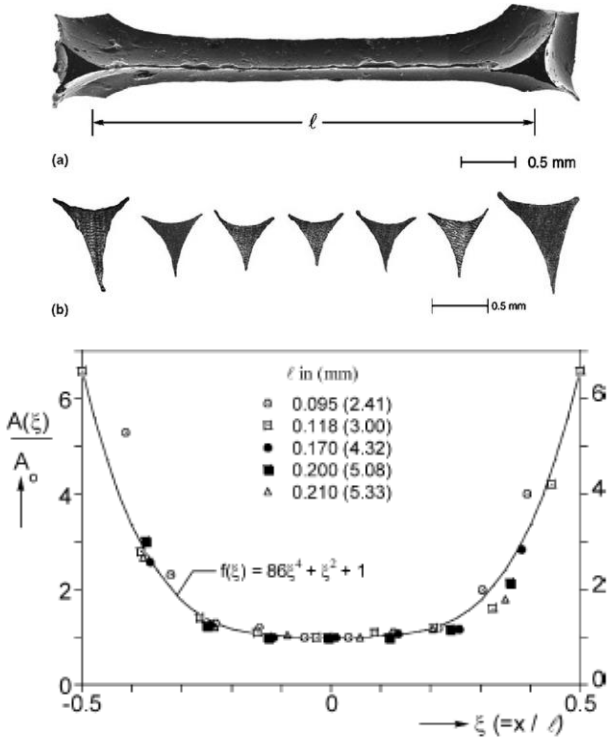

Strut cross section variation and mid-span cross-sectional area of a polyurethane foam; Gong et al 2004

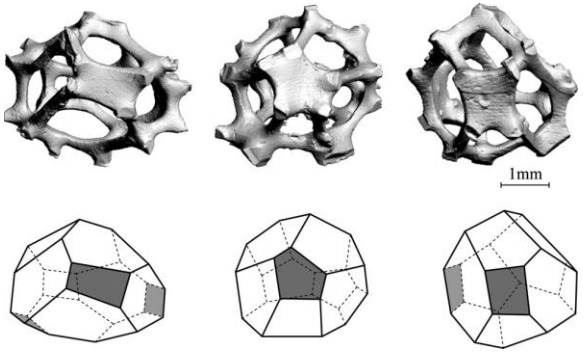

Closing of faces in metallic foam manufactured by investment casting; Gong et al 2004

Variation of relative density of the foam with varying cross section profile: plateau, triangular, casting convex triangular and circular (used in most models); Duocel™ by ERG

DN-RSA is able to incorporate these variations by modifying the “Plateau” function O_P according to the domain using DN_3 and DN_4.

Open foam materials

- Metallic open foams
  - Low density
  - Novel physical, mechanical and acoustic properties.
  - Offer potential for lightweight structures, with high stiffness and energy absorption capability.
  - With advancing manufacturing capabilities, they are becoming more affordable.
- Properties and applications results from chemical and physical properties of the bulk material and cell structure.
- Ability to model 3D foams based on actual foam samples
  - Helps in characterization
  - Stochastic approaches and multi-scale mechanics used to simulate the behavior

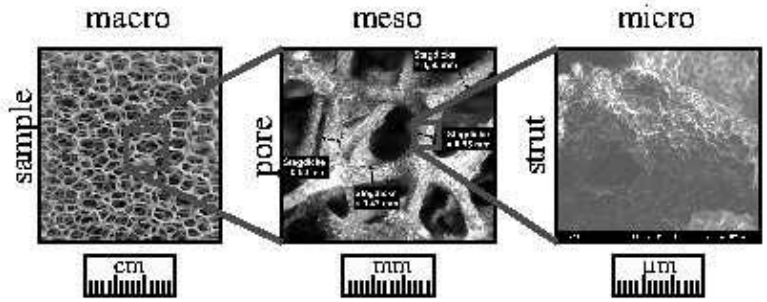

Jung & Diebels 2014

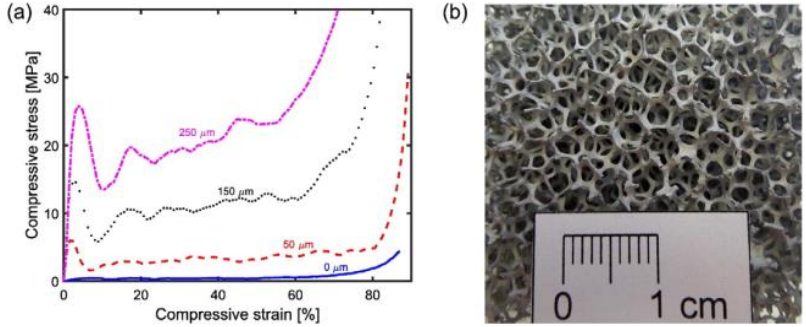

Jung et al 2015

Open foam properties

- Manufacturing (Zhou et al 2002)
  - PU foam → phenomenon of bubble expansion
  - Metallic foam → PU foams + casting/ electrodeposition
- Plateau's law (Sonon et al 2015)
  - Soap bubble → Plateau's law, Surface energy minimization
    - Constant mean curvature of each face
    - 3 faces meet at 120^0, equal dihedral angles
    - 4 edges join at equal tetrahedral angles (109.47^0)

Cross section of the struts of open-cell foam commercially manufactured by ERG under Duocel trademark; percentage refers to the resulting relative densty

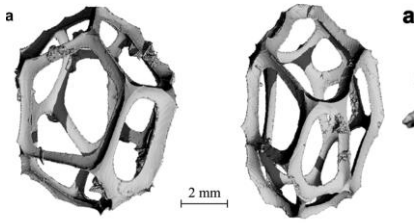

PU foam structure with concave triangular strut cross section

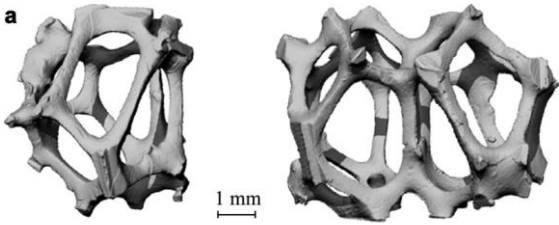

Aluminium foam structure with triangular strut cross section

Jang et al (2008)

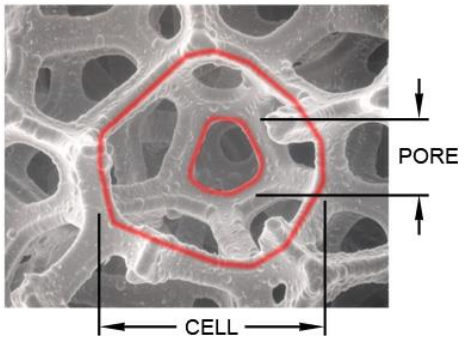

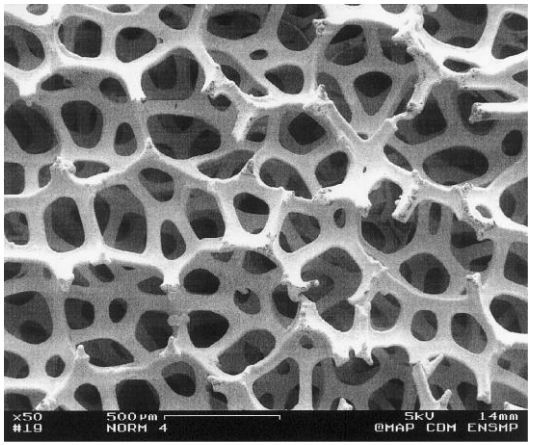

Nickel open-cell foam; Badiche et al (2000)

Numerical approach

- Regular models
  - Kelvin's tetrakaidecahedra (1887)
  - Weaire-Phelan cell (1993)
- Tessellations of sphere packing distribution – Laguerre tessellations
  - Sphere packing generation
    - Concurrent or force-biased approach (Ex, Stroeven 1996)
    - Sequential approach (Ex, RSA, Cooper 1988)
  - Tessellation generated by methods like convex hull (QHull, Barer et al 1996)
  - Morphological parameters like face-by-cell count, edge-by-face count, interior angles match very well

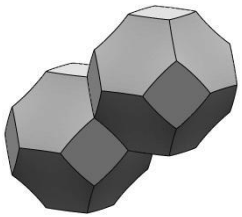

Kelvin cell

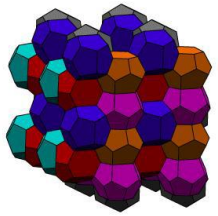

Weaire-Phelan modification

- Too regular
- Fail to represent non-uniform bubble sizes and out-of-equilibrium solid foams.

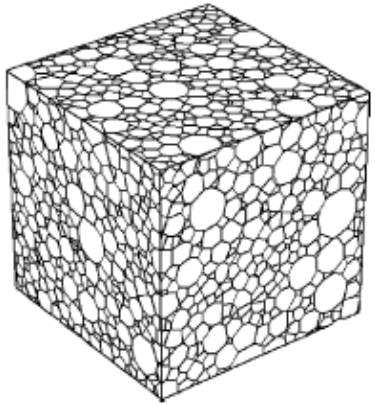

Random close packing of spheres based Laguerre Voronoï diagram (Fan et al 2004)

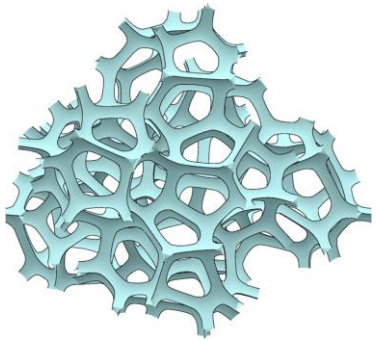

Soap bubble based model by Surface Evolver (Jang et al 2008). This process is complex and time-processer intensive

DN-RSA based packing generation

- Method to generate random arbitrary shaped inclusion packing based on distance neighbors (Sonon 2012)
  - Packing with no constraints between individual inclusions – Random sequential addition (RSA)
  - Constraints based on distance from nearest neighbors to generate the most optimal packing – DN-RSA
  - Limit of vanishing discretization size → Most optimal packing
  - Computational cost of the method is linear due to the control on neighboring distances
  - Can generate periodic packings as well as packings with free boundaries
  - Packing fraction of the spheres and distribution of the volumes of the spheres can be controlled to obtain a wide range of packings

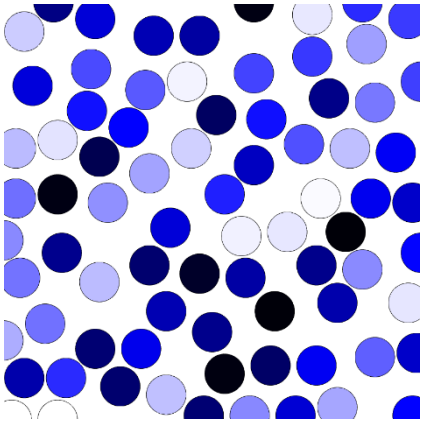

RSA packing

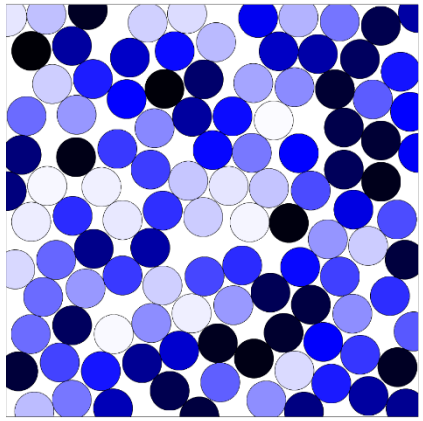

DN-RSA packing

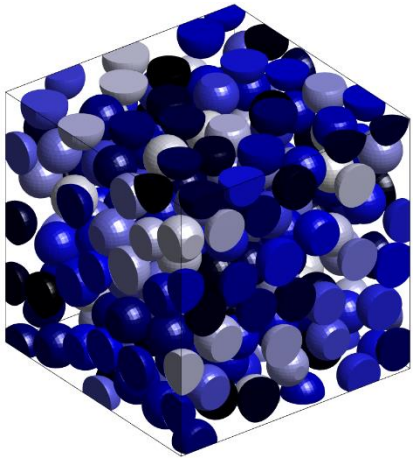

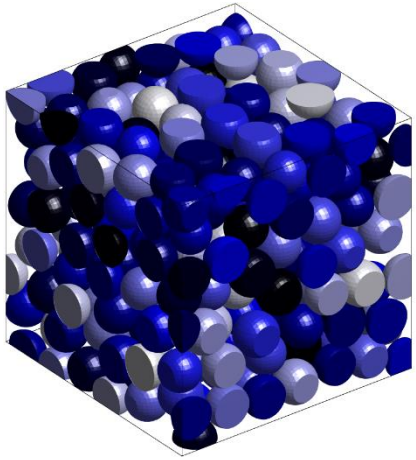

Open foam morphology

- Plateau borders in liquid foams form at the intersection of three films. Thus we combine the 3 first neighbor distance functions.
- “Plateau” Level set function
  - $O_P(\boldsymbol{x}) = \frac{DN_3(\boldsymbol{x})+DN_2(\boldsymbol{x})}{2} - DN_1(\boldsymbol{x})$
- Function consists of triangles with vertex lying on the tessellation cell boundaries.
- Thus, we can extract plateau border like geometry through
  - $O_P(\boldsymbol{x}) - t = 0$
  - Parameter t used to control thickness of extracted borders

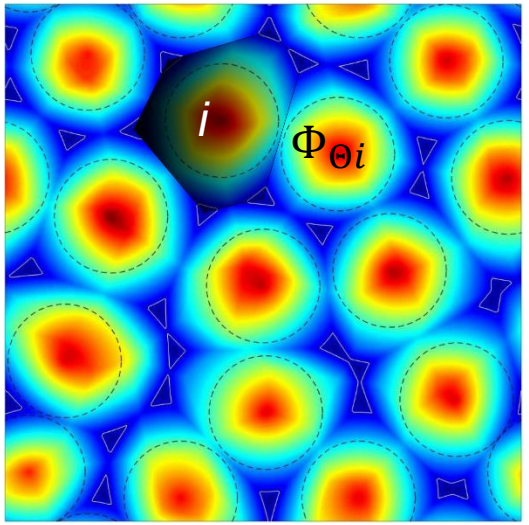

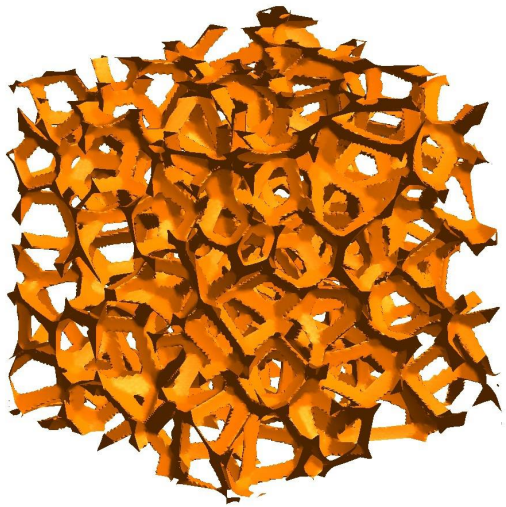

Open foam model with sharp edge using DN-RSA

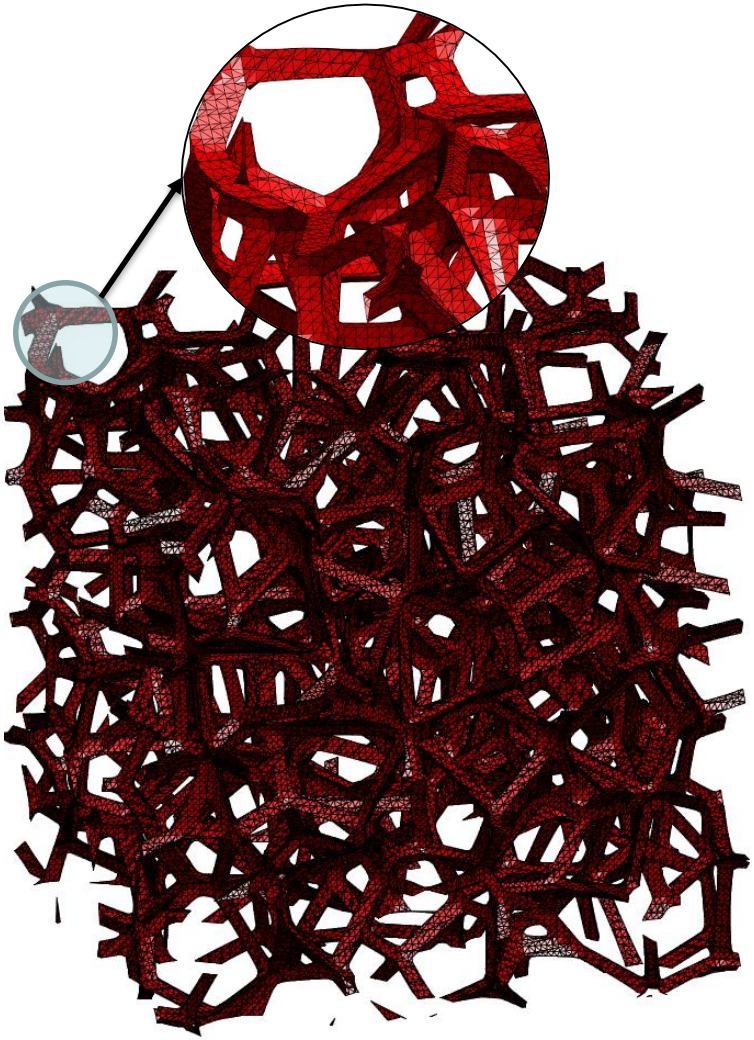

Assembly of all inclusions after sharp edge extraction

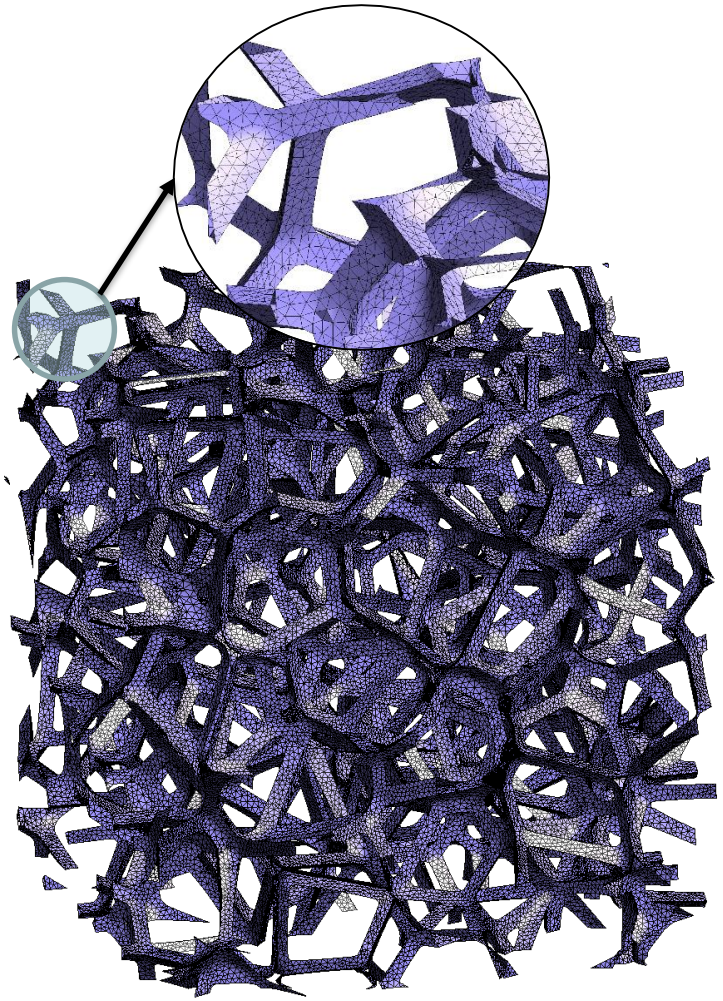

Assembly of all inclusions after remeshing, the surface elements have been processed to make the mesh more uniform

Morphology Characterization

Comparison between QHull Laguerre model and DN-RSA model

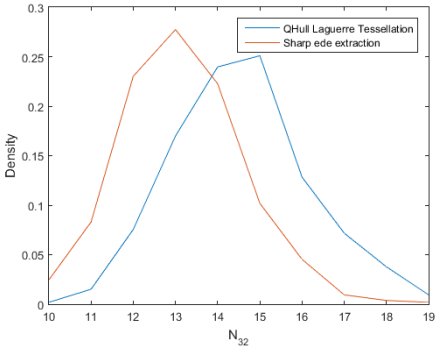

Comparison between Al foam sample, QHull Laguerre model and Surface Evolver based model fitted to Al foam; Vecchio et al 2016

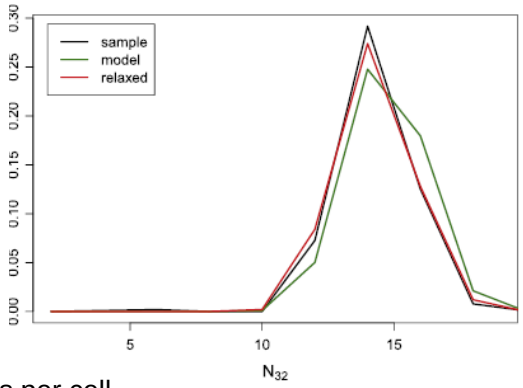

No. of faces per cell

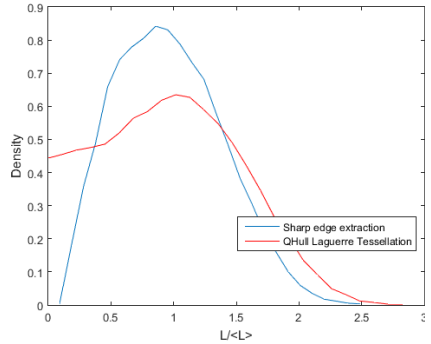

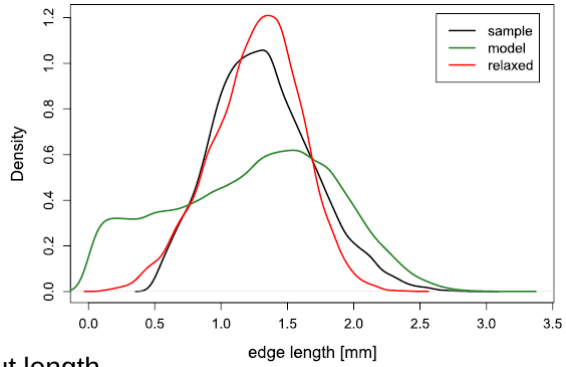

Strut length

- Classical Approach – Using the triangulated surfaces extracted from level set contouring
- Implicit approach – Using the calculated functions like NN_k, DN_k, O_P, etc

Typical high values found in Laguerre tessellations from QHull not obtained due to limitations of the discretization grid.

Strut length distribution from DN-RSA in comparison with QHull Laguerre tessellations show that the short edges get absorbed by the sharp edge extraction technique, mimicking the process of model extraction from (Van der Burg et al 1997)

Linear elastic analysis : Sample

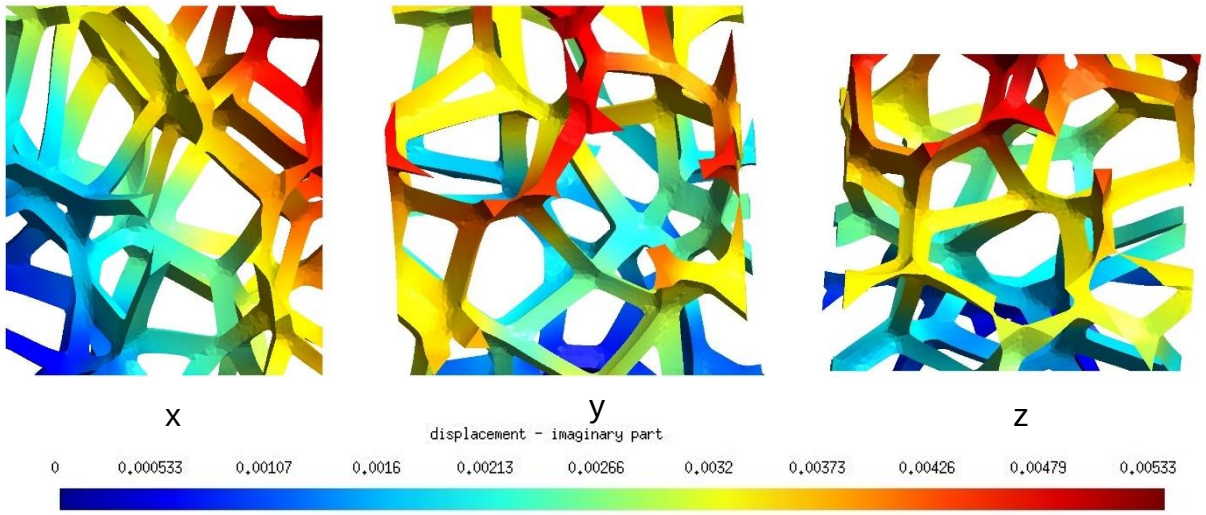

- Displacement analysis of an RVE of a foam generated using DN-RSA, the RVE is under tensile and shear stress.
- This shows the convenience of importing the RVE generated from DN-RSA to the solvers available with CM3 group to generate larger sized RVEs as Stochastic volume elements and analyze using multiscale techniques